Light harvesting antenna on an amyloid scaffold†

Yan Liang,[a] Peng Guo,[b] Sai Venkatesh Pingali,[c] Suzette Pabit,[b] Pappannan Thiyagarajan,*[c] Keith M. Berland*[b] and David G. Lynn*[a]

Received (in Cambridge, UK) 19th August 2008, Accepted 9th October 2008
First published as an Advance Article on the web 7th November 2008
DOI: 10.1039/b814262a

A pigment array has been constructed within a paracrystalline amyloid nanotube and Förster energy transfer along the nanotube surface has been demonstrated to self-assembled acceptor dyes.

Nature's reaction centers and light-harvesting complexes have remarkable long-range order in their pigment assemblies.[1–6] Artificial light harvesting complexes and reaction centers have either taken advantage of this natural ordering[7–9] by reconstructing arrays in synthetic lipid bilayer liposomes,[4,10–12] or by designing polymeric assemblies that order the pigments.[13–15] Here we exploit paracrystalline amyloid self-assembly[16] to construct pigment arrays on a new peptide nanotube scaffold and use Förster resonance energy transfer[17] measurements to probe the resulting pigment arrays.

Aβ(16–22), the seven-residue amyloid-β segment Ac-KLVFFAE-NH2, self-assembles into soluble amyloid nanotubes in CH_3CN–H_2O (2 : 3, v/v) with 0.1% TFA (Fig. 1(a)).[16] These Aβ(16–22) nanotubes maintain antiparallel one-residue shifted β-sheet bilayers within a cross-β architecture (Fig. 1(b)),[18] creating a nanotube surface that positions the peptide termini in a 5 Å × 10 Å rectangular pattern. Amyloid fibrils are sufficiently robust for functional molecular engineering,[19–22] and this patterned array across the nanotube surface appears suitable for light harvesting antenna construction.

The N- and C-terminal capped Aβ(16–22) contains a hydrophobic core, LVFFA, buttressed by polar Lys and Glu residues. Replacing the N-terminal cap with Rhodamine 110 (Rh110) *via* solid phase synthetic methods[16,18] yields Rh16–22. The additional overall positive charge in Rh16–22 increases its solubility in CH_3CN–H_2O (2 : 5, v/v) with 0.1% TFA, and the resulting fluorescent peptides readily form amyloid fibrils (Fig. 2(b)). Fourier transform infrared (FTIR) analysis confirmed an amide I band shift from 1639 to 1627 cm^{-1} (Fig. 2(d)), very similar to the assembled Aβ(16–22),[18] but with an additional rhodamine stretch at 1597 cm^{-1}. Wide angle X-ray scattering (WAXS) established the amyloid cross-β diffraction pattern with 5 Å (H-bonding) and broad 10 Å (lamination) bands (Fig. 2(c)), and the amide band at 1694 cm^{-1} was diagnostic of antiparallel β-sheets.[18] Therefore,

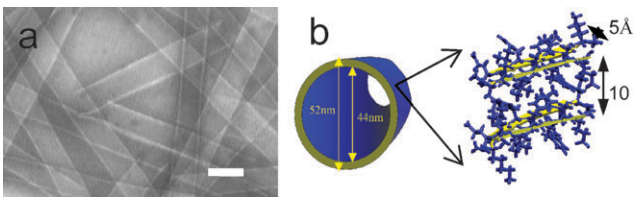

Fig. 1 Nanotubes formed by self-assembly of Aβ(16–22) in CH_3CN–H_2O (2 : 5, v/v) with 0.1% TFA; (a) TEM image, scale = 100 nm; (b) proposed structural model of the nanotubes. The inset shows the minimum cross-β repeating unit in the nanotube.[16,18]

rhodamine dyes can be successfully incorporated into the amyloid cross-β scaffold, but the self-assembled fluorescence fibers are too dense for detailed optical analyses.

As amyloids assemble through nucleation-dependent events, peptide co-assembly can be used to increase the range of accessible structures.[19,20] With Aβ(16–22) maintained as the dominant peptide to nucleate tube morphology, for example Aβ(16–22)/Rh16–22 at 250 : 1 molar ratio in a 1 mM total peptide solution in CH_3CN–H_2O (2 : 3, v/v) with 0.1% TFA, nanotube assemblies are readily observed by TEM (Fig. S1, ESI†). The overall morphology of the co-assemblies appear identical to the Aβ(16–22) nanotubes by TEM and the fluorescence seen by two-photon imaging (Fig. 3(a), excited at λ_{ex} = 780 nm) is homogeneously distributed across each nanotube.

To test directly for co-assembly, Rh110 alone was shown not to bind to the Aβ(16–22) nanotubes (Fig. 3(b)). Moreover, when [1-^{13}C]-F19 Rh16–22 at 0.15 mM, still well below its critical assembly concentration, was allowed to co-assembly with 1.5 mM Aβ(16–22), a distinct red-shifted shoulder on the main 1627 cm^{-1} amide I band appeared (Fig. 2(c)). This band is absent in the assembly lacking the ^{13}C label, and previous introduction of [1-^{13}C] labels into β-strands had been shown to split the amide I band through coupling of the ^{12}C and ^{13}C dipoles within the sheet.[23–25] For example, isotope-edited FTIR (IE-FTIR) of [1-^{13}C]-F19 incorporated Aβ(16–22) splits the main amide I band into components, 1640 and 1599 cm^{-1} (Fig. 2(c)),[18] and the shoulder seen in Fig. 2(c) is most consistent with this lower energy ^{13}C band. When taken together, these results confirmed the homogeneous co-assembly of Rh16–22 into the β-sheet array of the Aβ(16–22) nanotubes.

The demonstration of light harvesting by the incorporated Rh16–22 requires energy transfer to adjacent chromophores.[26] Taking advantage of the diagnostic Congo red staining[27] of amyloid nanotubes,[16,18] we explored the use of one of Rh110's FRET acceptors (Fig. 3(c)), Alexa 555 (A555), which maintains similar sulfate functionality on a planar aromatic nucleus. When mixed with mature Aβ(16–22) assemblies,

[a] *Center for Fundamental and Applied Molecular Evolution, Emory Center for BioInspired Renewable Energy, The Departments of Chemistry, Biology, Emory University, Atlanta, GA 30322, USA. E-mail: dlynn2@emory.edu*
[b] *Department of Physics, Emory University, Atlanta, GA 30322, USA*
[c] *Advanced Photon Source, Argonne National Laboratory, Argonne, IL 60439, USA*

† Electronic supplementary information (ESI) available: Experimental details, and TEM of the donor and acceptor with Aβ(16–22) nanotubes. See DOI: 10.1039/b814262a

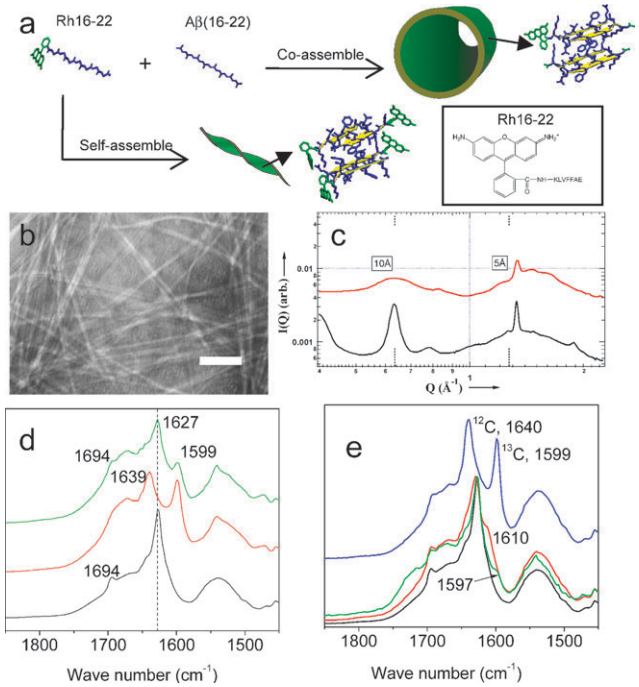

Fig. 2 Self-assembly of Rh16–22 and Aβ(16–22). (a) Rh16–22 assembled into fibers in CH_3CN–H_2O (2 : 5, v/v) with 0.1% TFA and the co-assembly of Rh16–22 with Aβ(16–22) into nanotubes in CH_3CN–H_2O (2 : 3, v/v) with 0.1% TFA, (b) TEM of Rh16–22 fibers, scale = 100 nm; (c) cross-β pattern of Rh16–22 fibers (red) and Aβ(16–22) tubes (black) detected by WAXS, (d) FTIR of Aβ(16–22) nanotubes (black), Rh16–22 fibers (green), and unassembled Rh16–22 (red); (e) IE-FTIR of [1-^{13}C]-F19 Aβ(16–22) (blue), Aβ(16–22) + [1-^{13}C]-F19 Rh16–22 (10 : 1) (red), Aβ(16–22) + Rh16–22 (10 : 1) (green), and Aβ(16–22) (black).

A555 indeed homogenously decorated the nanotube structure with no apparent morphological distortion of the architecture (Fig. 3(e), λ_{ex} = 980 nm). Likewise, when added to the Aβ(16–22)/Rh16–22 co-assembly, dye binding was also rapid and two photon fluorescence (data not shown) and lifetime imaging under the donor excitation wavelength (λ_{ex} = 780 nm) (Fig. 3(f)) was consistent with the binding to the intact nanotubes. As control, bound A555 is shown not to be excited efficiently at this wavelength (Fig. 3(d)).

Förster energy transfer efficiency with a single donor and acceptor has been assigned as inversely proportional to the sixth power of their separation,[17] and for Rh110 and A555 the assigned Förster radius R_0 is 6.6 nm. However, this single distance model is not sufficient to describe a pattern of multiple donors and acceptors across the 2D surface.[28] Given the initial 250 : 1 concentration ratio of Aβ(16–22) and Rh16–22, and assuming minimal impact of the attached chromophore on peptide incorporation frequency, every 10 laminates (10 nm) of 25 β-strands (12.5 nm) should have a single Rh16–22 peptide. When this nanotube pattern is further layered with A555 at a 4× lower concentration, the approximate spacing between the donor and acceptor is estimated to be on the order of 10 nm. When A555 is added to mature co-assembled Aβ(16–22)/Rh16–22 nanotubes to give the A555/Rh16–22/Aβ(16–22) assembly at a 1 : 4 : 1000 ratio with Aβ(16–22) at 0.5 mM, the center of the Rh16–22 lifetime distribution shifts from 3.7 to 3.3 ns (Fig. 4(a)). This corresponds to a FRET efficiency of 11%, calculated as $1 - (\tau'/\tau)$, where τ' is the Rh16–22 lifetime in the presence of A555, and τ is its lifetime in the absence.[29]

Under these conditions, only minimal direct excitation of the A555 acceptor should occur (Fig. 3(d)) and account for

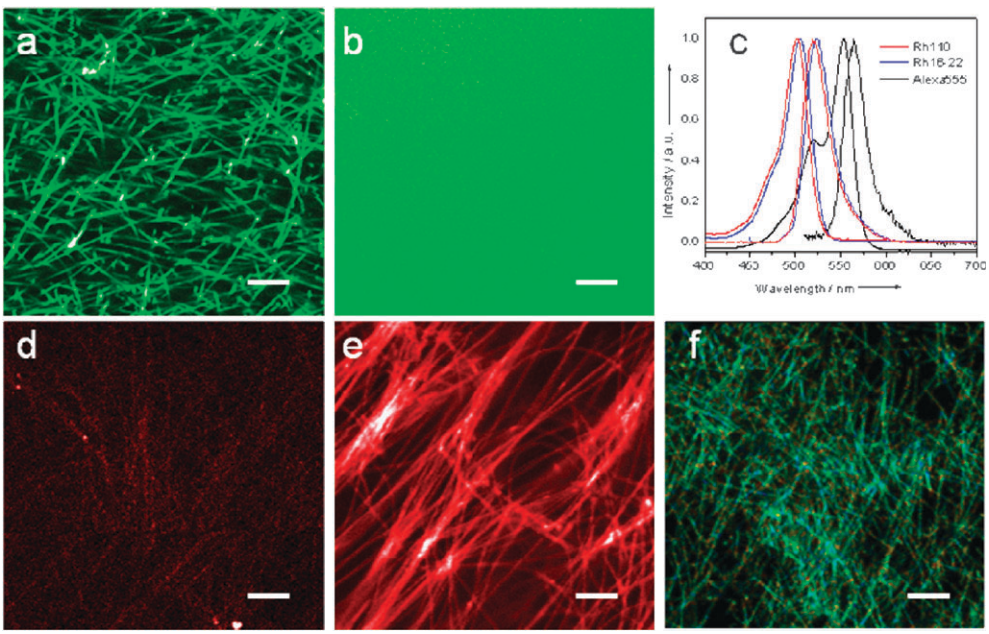

Fig. 3 Two-photon fluorescence imaging of donor and acceptor with Aβ(16–22) nanotubes. (a) Aβ(16–22) : Rh16–22 co-assembly (250 : 1 molar ratio, and λ_{ex} = 780 nm); (b) Aβ(16–22) mature nanotubes with Rh110, (250 : 1 molar ratio, and λ_{ex} = 780 nm); (c) single-photon absorbance and emission of Rh110 and Alexa 555 in CH_3CN–H_2O (2 : 3, v/v) with 0.1% TFA; (d) Aβ(16–22) mature nanotubes with A555 (1000 : 1 molar ratio, λ_{ex} = 780 nm). (e) Aβ(16–22) mature nanotubes with A555 (1000 : 1 molar ratio, λ_{ex} = 980 nm); (f) lifetime image of Aβ(16–22) : Rh16–22 fluorescence nanotubes (250 : 1 molar ratio, and λ_{ex} = 780 nm). Image scale = 5 μm.

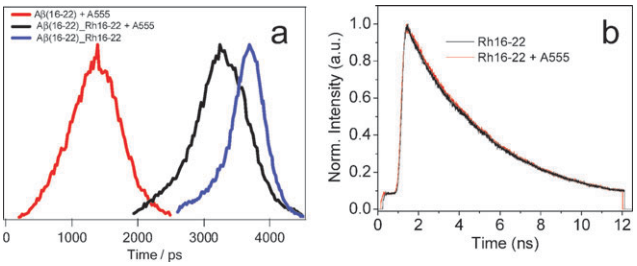

Fig. 4 FRET lifetime analysis. (a) Lifetime distribution of A555 (red) with mature Aβ(16–22) nanotubes, and Aβ(16–22)/Rh16–22 fluorescence nanotubes in the presence (black) and absence (blue) of A555; (b) representative lifetime decays of Rh16–22 and a mixture of Rh16–22 and A555 in the absence of Aβ(16–22) nanotubes in CH_3CN–H_2O (2 : 3, v/v) with 0.1% TFA.

less than 2% of the total signal in the FRET samples. To further rule out the influence of direct acceptor excitation on the measured FRET efficiency, we modeled what the average lifetime would be for the mixture of the two dyes with 2% of the total intensity arising from direct acceptor excitation when fit to a single exponential decay. The average fluorescence lifetime of Rh16–22 in Aβ(16–22) nanotubes is 3.7 ns, and the average lifetime of A555 on Aβ(16–22) nanotubes is 1.3 ns. For the peak A555 signal at 2% of the Rh110 signal, the lifetime would shift only to 3.6 ns, significantly longer than the measured lifetime of 3.3 ns. In addition, there is no energy transfer between Rh16–22 and A555 in solution when they are not co-assembled into Aβ(16–22) tubes (Fig. 4(b)). Preliminary experiments suggest indeed that a further increase in FRET efficiency can be achieved by increasing the ratio of the donor along the amyloid scaffold. Taken together, these results are most consistent with the functionalized Rh16–22 peptides being randomly incorporated as the Aβ(16–22) nanotubes assemble and demonstrate the light harvesting ability of this amyloid cross-β scaffold.

This demonstrated ability to assemble strong chromophores across the paracrystalline amyloid network allows for precise ordering along the inner and outer compartment walls of an all protein nanotube. Given the dimensions of the array, it should now be possible to incorporate further molecular recognition elements, construct higher order arrays,[30] and even include elements for energy and electron separation reactions. Accordingly, this extension of amyloid self-assembly to more precise supramolecular arrays containing functional pigments provides a critical first step in constructing a self-assembling nanoscale scaffold for new bio-inspired antenna and photosynthetic devices.

The work benefited from the Apkarian Microscopy Center at EU, assistance from Dr Soenke Seifert at the APS under contract number DE-AC02-06CH11357 between UChicago Argonne, LLC and the Department of Energy, support from DOE (ER15377), NSF (CRC-CHE-0404677), and NSF (CBC-CHE-0739189), and for CD instrumentation from NSF (CHE-0131013).

Notes and references

1 J. P. Allen, G. Feher, T. O. Yeates, H. Komiya and D. C. Rees, *Proc. Natl. Acad. Sci. USA*, 1987, **84**, 5730–5734.
2 J. P. Allen and J. C. Williams, *FEBS Lett.*, 1998, **438**, 5–9.
3 A. Damjanovic, I. Kosztin, U. Kleinekathofer and K. Schulten, *Phys. Rev. E*, 2002, **65**, 31919–31953.
4 M. R. Jones, *Prog. Lipid Res.*, 2007, **46**, 56–87.
5 J. Deisenhofer, O. Epp, K. Miki, R. Huber and H. Michel, *J. Mol. Biol.*, 1984, **180**, 385–398.
6 C. H. Chang, O. El-Kabbani, D. Tiede, J. Norris and M. Schiffer, *Biochemistry*, 1991, **30**, 5352–5360.
7 J. Goca, M. Harab, T. Tateishia and J. Miyake, *J. Photochem. Photobiol. A: Chemistry*, 1996, **93**, 137–144.
8 K. Iida, H. Kiriyama, A. Fukai, W. N. Konings and M. Nango, *Langmuir*, 2001, **17**, 2821–2827.
9 T. Dewa, *Selective e-J. Surf. Sci. Nanotechnol.*, 2005, **3**, 145–150.
10 T. Páli, G. Garab, L. I. Horváth and Z. Kóta, *Cell. Mol. Life Sci.*, 2003, **60**, 1591–1606.
11 S. Bahatyrova, R. N. Frese, C. A. Siebert, J. D. Olsen, K. O. v. d. Werf, R. v. Grondelle, R. A. Niederman, P. A. Bullough, C. Otto and N. Hunter, *Nature*, 2004, **430**, 1058–1062.
12 S. Scheuring, J. N. Sturgis, V. Prima, A. Bernadac, D. Levy and J. L. Rigaud, *Proc. Natl. Acad. Sci. USA*, 2004, **101**, 11293–11297.
13 S. E. Webber, *Chem. Rev.*, 1990, **90**, 1469–1482.
14 D. M. Watkins and M. A. Fox, *Desk Reference of Functional Polymers Syntheses and Applications*, 1997, ch. 4, pp. 549–566.
15 T. Hasobe, K. Saito, P. V. Kamat, V. Troiani, H. Qiu, N. Solladie, K. S. Kim, J. K. Park, D. Kim, F. D'Souza and S. Fukuzumi, *J. Mater. Chem.*, 2007, **17**, 4160–4170.
16 K. Lu, J. Jacob, P. Thiyagarajan, V. P. Conticello and D. G. Lynn, *J. Am. Chem. Soc.*, 2003, **125**, 6391–6393.
17 B. W. v. d. Meer, *Resonance Energy Transfer: Theory and Data*, VCH, New York, 1994; K. B. Towles, A. C. Brown, S. P. Wrenn and N. Dan, *Biophys. J.*, 2007, **93**, 655–667.
18 A. K. Mehta, K. Lu, W. S. Childers, Y. Liang, S. Dublin, J. Dong, J. S. Snyder, S. V. Pingali, P. Thiyagarajan and D. G. Lynn, *J. Am. Chem. Soc.*, 2008, **130**, 9829–9835.
19 S. Gilead and E. Gazit, *Supramol. Chem.*, 2005, **17**, 87–92.
20 D. Hamada, I. Yanagihara and K. Tsumoto, *Trends Biotechnol.*, 2004, **22**, 93–97.
21 C. E. MacPhee and C. M. Dobson, *J. Am. Chem. Soc.*, 2000, **122**, 12707–12713.
22 H. Kodama, S. Matsumura, T. Yamashitaa and H. Mihara, *Chem. Commun.*, 2004, 2876–2877.
23 H. Hiramatsu and T. Kitagawa, *Biochim. Biophys. Acta*, 2005, **1753**, 100–107.
24 S. A. Petty and S. M. Decatur, *J. Am. Chem. Soc.*, 2005, **127**, 13488–13489.
25 C. Paul and P. H. Axelsen, *J. Am. Chem. Soc.*, 2005, **127**, 5754–5755.
26 R. A. Miller, A. D. Presley and M. B. Francis, *J. Am. Chem. Soc.*, 2007, **129**, 3104–3109; Y. -Z. Ma, R. A. Miller, G. R. Fleming and M. B. Francis, *J. Phys. Chem.*, 2008, **112**, 6887–6892.
27 M. T. Elghetany, A. Saleem and K. Barr, *Ann. Clin. Lab. Sci.*, 1989, **19**, 190–195.
28 T. G. Dewey and G. G. Hammes, *Biophys. J.*, 1980, **32**, 1023–1036; B. Corry, D. Jayatilaka and P. Rigbyy, *Biophys. J.*, 2005, **89**, 3822–3836.
29 H. Wallrabe and A. Periasamy, *Curr. Opin. Biotechnol.*, 2005, **16**, 19–27.
30 K. Lu, L. Guo, A. K. Mehta, W. S. Childers, S. N. Dublin, V. P. Conticello, P. Thiyagarajan, R. P. Apkarian and D. G. Lynn, *Chem. Commun.*, 2007, 2729–2731.

